

Preprint ЕФИ-868(19)-86

ԵՐԵՎԱՆԻ ՖԻԶԻԿԱՅԻ ԻՆՍՏԻՏՈՒՏ
ЕРЕВАНСКИЙ ФИЗИЧЕСКИЙ ИНСТИТУТ

Yu.G. SHAKHNAZARYAN

$e^+e^- \rightarrow q\bar{q}g$ PROCESS CROSS SECTION TRANSVERSE
MOMENTUM DISTRIBUTION FOR HEAVY QUARKS

ЦНИИатоминформ

ЕРЕВАН-1986

ՇԱՀՆԱԶԱՐՅԱՆ ՑՈՒԳ.

$e^+e^- \rightarrow q\bar{q}$ ԴՐՈՑԵՍԻ ԿՏՐՎԱԾՔԻ ՔԱՇԽՈՒՄԸ ԸՍՏ ԼԱՅՆԱԿԻ
ԽՐԴՈՒԼՍԻ՝ ԾԱՆՐ ԲՎԱՐԿՆԵՐԻ ՀԱՄԱՐ

Քմանտային քրոմոդինամիկայի շրջանակներում հետազոտված է ծանր բվարկների զանգվածի հաշվառման ազդեցությունը $e^+e^- \rightarrow q\bar{q}$ եռափունջ պրոցեսի կտրվածքի՝ ըստ T /առավել մեծ էներգիա ունեցող պարտոնի իմպուլս/ և α_s /մյուս երկու պարտոնների \bar{T} առանցքի նկատմամբ լայնակի իմպուլս/ փոփոխականների Քաշխման վրա: Ցույց է տրված, որ ստացվող արդյունքները էապես կախված են քմարկի զանգվածից: Զանգվածի հաշվառումը Բերում է ոչ միայն α_s -ի փոփոխման տիրույթի զգալի ընդլայնմանը՝ զանգվածը հաշվի չառնելու դեպքի համեմատ, և այդ տիրույթի տեղաշարժմանը դեպի α_s -ի փոքր արժեքները, այլև $d^2\sigma/dT d\alpha_s$ կտրվածքի α_s -կախվածությունը նկարագրող կորերի վրա կառուցվածքների առաջագմանը:

Երևանի Ֆիզիկայի ինստիտուտ

Երևան 1986

Yu.G. SHAKHNAZARYAN

$e^+e^- \rightarrow q\bar{q}g$ PROCESS CROSS SECTION TRANSVERSE
MOMENTUM DISTRIBUTION FOR HEAVY QUARKS

In QCD framework the influence of taking the mass of heavy quarks into account on the distribution over the value T (thrust, the momentum of the most energetic parton) and on transverse to \vec{T} axis momentum x_{\perp} of each of two other partons in the process $e^+e^- \rightarrow q\bar{q}g$, responsible for three-jet events in e^+e^- annihilation, is investigated. It is shown that the account of quark mass has a considerable effect on theory predictions. This leads to significant widening of variation range of x_{\perp} as compared with the massless case, to the shift of this range towards small values of x_{\perp} and also to structures in curves describing the dependence of the cross section $d^2\sigma/dTdx_{\perp}$ on x_{\perp} .

Yerevan Physics Institute

Yerevan 1986

Ю.Г.ШАХНАЗАРЯН

РАСПРЕДЕЛЕНИЕ ПО ПОПЕРЕЧНОМУ ИМПУЛЬСУ СЕЧЕНИЯ
ПРОЦЕССА $e^+e^- \rightarrow q\bar{q}g$ ДЛЯ ТЯЖЕЛЫХ КВАРКОВ

В рамках КДП исследовано влияние учета массы тяжелой кварков на распределение по величине T (импульсу наиболее энергичного партона) и поперечному относительно оси \vec{T} импульсу x_1 каждого из двух других партонов в процессе $e^+e^- \rightarrow q\bar{q}g$, ответственном за трехструйные события в e^+e^- -аннигиляциях. Показано, что масса кварка оказывает заметное влияние на предсказания теории. Учет массы приводит не только к значительному расширению области изменения x_1 по сравнению с безмассовым случаем и смещению этой области в сторону меньших значений x_1 , но и к появлению структур у кривых, описывающих зависимость $d^2\sigma / dT dx_1$ от x_1 .

Ереванский физический институт

Ереван 1986

It is known that the hadron production in e^+e^- annihilation at high energies is of a jet nature. According to modern views primarily a quark-antiquark pair is formed which then decays into hadrons flying in opposite directions in the form of two jets. Hadrons in jets are experimentally found to have a limited transverse momentum of ~ 300 MeV/c relative to jet axis independent of energy. That is why the jets will be narrowed and become more distinct with increasing reaction energy as the multiplicity of the produced hadrons grows only logarithmically here.

However, at rather high energies, in e^+e^- annihilation events with large transverse momenta are observed, though, not so frequently. They are due to bremsstrahlung of hard gluon in the process $e^+e^- \rightarrow q\bar{q}g$. Gluon also fragments into hadrons, and a planar three-jet event is experimentally observed as a result. To describe the mentioned process in QCD and compare theory with experiment, usually the so-called infrared-stable variables are used. Among them is, in particular, the thrust T [1,2] and transverse to \vec{T} axis momentum x_\perp [3] of each of two other jets.

In Ref.[4] the differential over variables T and x_\perp cross section of the three-jet process $e^+e^- \rightarrow q\bar{q}g$ has

been calculated in the first order of QCD, the mass of quark being ignored. As at energies achievable on modern storage rings the mass of c and b quarks and all the more, that of t quark can appreciably change the results, in the present work an analogous consideration with heavy quarks is made. Such a generalization is not trivial but a complicated one.

The differential cross section of the process $e^+e^- \rightarrow q\bar{q}g$ with heavy quarks and non-polarized primary particles, after summation over colours and integration over angles has the form (see, e.g., Refs[5-8]):

$$\frac{d^2\sigma}{dx'_1 dx'_2} = \frac{8\alpha^2\alpha_s Q^2}{3S} \rho(x'_1, x'_2, x_3),$$

$$\rho(x'_1, x'_2, x_3) \equiv \frac{1}{(1-x'_1)(1-x'_2)} \left\{ x_1'^2 + x_2'^2 + \eta \left[1 - x_3 - \frac{1}{2} \left(1 + \frac{1}{2} \eta \right) \frac{x_3^2}{(1-x'_1)(1-x'_2)} \right] \right\} \quad (1)$$

Here S is the squared total energy of reaction, $\eta = 4m^2/S$, m and Q are the mass and the charge of quark (in the units of e). Variables $\vec{x}_n = 2\vec{P}_n/\sqrt{S}$ and $x'_n = 2E_n/\sqrt{S}$ determine the dimensionless momentum and dimensionless energy of n parton, respectively ($n = 1, 2, 3$, accordingly for q, \bar{q}, g), and relate as

$$x'_{1,2} = (\vec{x}_{1,2}^2 + \eta)^{1/2}, \quad x'_3 = x_3.$$

Taking $x_i \geq x_j \geq x_k$, let us determine variables, through which the original cross section (1) must be expressed

$$T = \max(x_1, x_2, x_3) = \max(x_i, x_j, x_k) = x_i, \quad (2)$$

$$x_1 = x_j \sin \theta_{ij} = x_k \sin \theta_{ik} = \frac{1}{x_i} [4(1-x'_i)(1-x'_j)(1-x'_k) - \eta x_3^2]^{1/2}.$$

To pass on to these variables in the cross section (1), let us divide the phase space into the regions [8]

$$\text{I. } x_1 \geq x_2 \geq x_3, \quad \text{II. } x_1 \geq x_3 \geq x_2, \quad \text{III. } x_3 \geq x_1 \geq x_2. \quad (3)$$

In the region I at $1_0 \leq 1 \leq T_B$, x_3 varies in the range of $2(1-T') \leq x_3 \leq [(2-T')^2 - \eta]/2(2-T')$ and, for other values of $T_B \leq T \leq T_A$ - in the range of $2(1-T') \leq x_3 \leq 2(1-T')/(2-T-T')$, where $T_0 = -2/3 + 4(1-3\eta/4)^{1/2}/3$ is the minimal value of T for all the regions (3), $T_A = (1-\eta)^{1/2}$, $T_B \approx 1 - (3\eta/4)(1+\eta^2/4)$.

In the variables (T, x_{\perp}) the boundary $x_3 = 2(1-T')$ is determined by expression

$$x_{\perp} = \frac{2(1-T')}{T} (2T' - 1 - \eta)^{1/2} \equiv x_{\perp}^{(1)} \quad (4)$$

(curve 1 in Fig.1), the boundary $x_3 = [(2-T')^2 - \eta]/2(2-T')$ is determined by

$$x_{\perp} = \left[1 - T' - \frac{\eta}{4} + \frac{\eta^2}{4(2-T')^2} \right]^{1/2} \equiv x_{\perp}^{(2)} \quad (5)$$

(curve 2 in Fig.1), and on the boundary $x_3 = 2(1-T')/(2-T-T')$

$x_{\perp} = 0$. The solid lines in Fig.1 correspond to the value $\eta = 0.1$ which this parameter obtains, for instance, for δ quark at $\sqrt{s} \approx 30$ GeV.

In contrast to the massless case when the transverse momentum obtains its maximum and minimum values on the boundaries of admissible phase space [4], at taking the mass of quark into account, x_{\perp} obtains its maximum value

$$x_{\perp}^{\max} = \frac{2(1-T')}{[4(1-T') + \eta]^{1/2}} \equiv x_{\perp}^{(3)} \quad (6)$$

(curve 3 in Fig.1) at $x_3 = 2(1-T')(2-T')/[4(1-T') + \eta]$.

It is not difficult to check that at the fixed T the transverse momentum obtains the maximum value (6) not for all T but when

$$3T' - 2 - \eta \geq 0, \quad T' \geq \frac{2+\eta}{3}, \quad T \geq \frac{1}{3} [(4-\eta)(1-\eta)]^{1/2} \equiv T_K. \quad (7)$$

So, the phase space of region I in variables (T, x_1) is determined by

$$\begin{aligned} T_0 &\leq T \leq T_K, & x_1^{(2)} &\leq x_1 \leq x_1^{(1)}, \\ T_K &\leq T \leq T_B, & x_1^{(1)} &\leq x_1 \leq x_1^{(3)}, & x_1^{(2)} &\leq x_1 \leq x_1^{(3)}, \\ T_B &\leq T \leq T_A, & x_1^{(1)} &\leq x_1 \leq x_1^{(3)}, & 0 &\leq x_1 \leq x_1^{(3)}. \end{aligned} \quad (8)$$

The phase space shape strongly depends on the quark mass. In the massless case for all three regions (3) it has the form shown by dashed lines in Fig.1.

In the region II the variation range of T is $T_0 \leq T \leq T_B$. In the interval $T_0 \leq T \leq T_C$ the range of permissible values of x_3 is $[(2-T')^2 - \eta]/2(2-T') \leq x_3 \leq T$, while in the interval $T_C \leq T \leq T_B$ it is $[(2-T')^2 - \eta]/2(2-T') \leq x_3 \leq 2(1-T)/(2-T)$. $T_C = 2(1-\sqrt{\eta})/(2-\sqrt{\eta})$. The lower boundary of the x_3 variation range in the variables (T, x_1) is determined by (5) (curve 2 in Fig.1), the boundary $x_3 = T$ - by

$$x_1 = \frac{1}{T} [4(1-T')(1-T)(T+T'-1) - \eta T^2]^{1/2} \equiv x_1^{(4)} \quad (9)$$

(curve 4). At the other upper boundary $x_1 = 0$ as before. The maximum (9) in the region II is not achieved and the transverse momentum obtains its maximum and minimum values at the boundaries of the region.

So, the phase space in the region III is determined by

$$\begin{aligned} T_0 &\leq T \leq T_C, & x_1^{(4)} &\leq x_1 \leq x_1^{(2)}, \\ T_C &\leq T \leq T_B, & 0 &\leq x_1 \leq x_1^{(2)}. \end{aligned} \quad (10)$$

and is limited by the curves 2 and 4 and the abscissa between the points B and C (see Fig.1).

In the region III at the fixed T the function $x_1(x_1')$ obtains its maximum value

$$x_1^{\max} = (1-T-\eta)^{1/2} \equiv x_1^{(5)} \quad (11)$$

(curve 5 in Fig.1) at the point $x'_1 = 1 - T/2$. As x'_1 now varies in the range of $1 - T/2 \leq x'_1 \leq T'$ when $T_0 \leq T \leq T_C$ and in the range of $1 - T/2 \leq x'_1 \leq 1 - T/2 + [1 - \eta/(1 - T)]^{1/2} T/2$, when $T_C \leq T \leq T_D$, where $T_D = 1 - \eta$, then the maximum value (11) is achieved at the lower boundary and the minimum value (9) or

$x_\perp = 0$, depending on T , is achieved at the upper boundaries

$x'_1 = T'$ and $x'_1 = 1 - T/2 + [1 - \eta/(1 - T)]^{1/2} T/2$, respectively:

$$\begin{aligned} T_0 \leq T \leq T_C, & \quad x_\perp^{(4)} \leq x_\perp \leq x_\perp^{(5)}, \\ T_C \leq T \leq T_D, & \quad 0 \leq x_\perp \leq x_\perp^{(5)}. \end{aligned} \quad (12)$$

So, the phase space in the region III is limited by the curves 4 and 5 and by the axis $x_\perp = 0$ between the points 3 and D (see Fig.1).

Let us now come to variables T and x_\perp in the cross section (1). In the regions I and II one has

$$\begin{aligned} x_2'^{\pm} = 2 - T' - x_3^{\mp}, \quad x_3^{\pm} = \frac{2(1 - T')}{4(1 - T') + \eta} (2 - T' \pm T y_1), \\ y_1 \equiv \left[1 - \frac{4(1 - T') + \eta}{4(1 - T')^2} x_\perp^2 \right]^{1/2}, \end{aligned} \quad (13)$$

$$dx_1' dx_2' = \frac{T^2 x_\perp}{2T'(1 - T') y_1} dT dx_\perp,$$

and in the region III -

$$\begin{aligned} x_1'^{\pm} = x_2'^{\pm} = 1 - \frac{T}{2} (1 \mp y_2), \quad y_2 \equiv \left(1 - \frac{x_\perp^2 + \eta}{1 - T} \right)^{1/2}, \\ dx_1' dx_2' = dx_1' dx_3 = \frac{T x_\perp}{2(1 - T) y_2} dT dx_\perp. \end{aligned} \quad (14)$$

In virtue of the conservation laws, to the values $x_2'^{\pm}$ correspond x_3^{\mp} for the first two regions. It is not difficult to see that always $x_2^+ > x_3^-$, regardless of T and x_\perp , while the condition $x_3^+ > x_2^-$ is satisfied only when $x_\perp < x_\perp^{(2)}$. That is why in the region I where according to (3) $x_2 \geq x_3$,

It is necessary to consider together with the distribution

$$\rho(T; x_2^+, x_3^-) \text{ also } \rho(T; x_2^-, x_3^+) \text{ for the values of } x_1 \geq x_1^{(2)}.$$

As these are two branches of the same function, they intersect

at the point $x_2^+ = x_2^-$ ($x_3^- = x_3^+$) where $y_1 = 0$, which is

realized at the value of $x_1 = x_1^{(3)}$. At $\eta = 0$ this is the

transition point between the regions I and II. With regard

to the quark mass such transition, which should take place at

$$x_2 = x_3, \text{ is realized at } x_1 = x_1^{(2)}.$$

Normalizing the cross section (1) to the total cross section

$$\sigma_{\mu\mu} = 4\pi\alpha^2/3s \text{ of the process } e^+e^- \rightarrow \mu^+\mu^-, \text{ and taking into}$$

account the regions obtained from (3) by substitutions $x_1 \rightleftharpoons x_2$,

the differential cross section for the regions I and II will

have the form

$$\frac{1}{\sigma_{\mu\mu}} \frac{d^2\sigma_{I,II}}{dTdx_1} = 2 \frac{\alpha_s}{\pi} Q^2 \frac{T^2 x_1}{T'(1-T')y_1} \rho_{I,II}. \quad (15)$$

For the region I

$$\rho_I = \rho(T; x_2^+, x_3^-) + \rho(T; x_2^-, x_3^+),$$

$\rho(T; x_2^+, x_3^-)$ describing the distribution for the values

$$T_K \leq T \leq T_L, \quad x_1^{(1)} \leq x_1 \leq x_1^{(3)}, \quad (16)$$

and $\rho(T; x_2^-, x_3^+)$ - for the values

$$\begin{aligned} T_0 \leq T \leq T_K, & \quad x_1^{(2)} \leq x_1 \leq x_1^{(1)}, \\ T_K \leq T \leq T_B, & \quad x_1^{(2)} \leq x_1 \leq x_1^{(3)}, \\ T_B \leq T \leq T_A, & \quad 0 \leq x_1 \leq x_1^{(3)}. \end{aligned} \quad (17)$$

In the region II, where according to (3) $x_3 \geq x_2$, in virtue of the above said one has

$$\rho_{II} = \rho(T; x_2^-, x_3^+)$$

for all admissible values (10).

Thus, some events with $x_1 \geq x_1^{(2)}$ being described by the function $\rho(\tau, x_2^-, x_3^+)$ as well as all the events described by the function $\rho(\tau, x_2^+, x_3^-)$ refer to the region I. In consequence, the cross section in the region II breaks at $x_1 = x_1^{(2)}$ and the cross section in the region I makes a jump, shown by a dashed line in Fig.2. If at $\eta \neq 0$ the function $\rho(\tau, x_2^-, x_3^+)$ describes only events in the region II, then the curves I and II in Fig.2 would intersect at the point $x_1 = x_1^{(3)}(\eta)$ as it is in the case of $\eta = 0$.

The differential cross section in the region III has the form

$$\frac{1}{\sigma_{\mu\mu}} \frac{d^2\sigma_{\text{III}}}{d\tau dx_1} = 2 \frac{\alpha_s}{\pi} Q^2 \frac{\tau x_1}{(1-\tau)y_2} \rho_{\text{III}}, \quad (18)$$

where

$$\rho_{\text{III}} = \rho(x_1^+, x_2^-, \tau)$$

for all the values of (12).

On the boundary $x_1 = x_3 = \tau$ of the regions II and III, corresponding to $x_1 = x_1^{(4)}$, $\rho(\tau, x_2^-, x_3^+) = \rho(x_1^+, x_2^-, \tau)$ takes place. However, due to the difference between the phase volumes of the regions II and III, the corresponding curves in Fig.2 at $\eta = 0.1$ do not intersect.

In Fig.2 at some admissible values of η the curves of $(4 \frac{\alpha_s}{\pi} Q^2 \sigma_{\mu\mu})^{-1} d^2\sigma/dx_1 dy$ as a function of x_1 in the regions I-III for the certain value $\tau = 0.8$ are given to illustrate to what quantitative changes leads the taking of the quark mass into account. Events with such τ can be initiated by both, light and heavy quarks, that is why on this example one can clearly see how much the taking of the quark mass into account affects

the theory predictions.

As it is seen in Fig.2, all the curves for the regions I-III shift to the left, to the smaller values of x_{\perp} with the increasing η . At $\eta = 0$ in all regions the transverse momentum varies in the same range, while it is not so at $\eta \neq 0$, the regions II and III noticeably expanding over x_{\perp} at the same time (also see Fig.1). Discontinuities on the curves in the region I at $\eta \neq 0$ are due to the fact, that beginning from a certain value of the transverse momentum at a given η ($x_{\perp} \geq x_{\perp}^{(2)} \approx 0.342$ at $\eta = 0.1$ and $x_{\perp} \geq x_{\perp}^{(2)} \approx 0.205$ at $\eta = 0.2$) some events, which at small values of x_{\perp} contributed to the region II, now do to the region I. It follows from the curves shown in Fig.2 that there is a rather wide range of the values of x_{\perp} at $\eta = 0.1$ ($0.124 \approx x_{\perp}^{(4)} \leq x_{\perp} \leq x_{\perp}^{(1)} \approx 0.275$) where the gluon jet can be either of intermediate energy as compared with q and \bar{q} jets, or the most energetic one. Drawing nearer to the upper boundary of η first of all disappear the events in the region III, and then in the region II too. So, in the considered case of $T = 0.8$ at $\eta = 0.2$ there are no events in the region III and at $\eta \approx 0.26$ - in the region II as well.

Using the expressions (15)-(18) it is easy to obtain the summary distribution in variables T and x_{\perp} for the process we are interested in:

$$\frac{1}{6_{\mu\mu}} \frac{d^2\mathcal{G}}{dT dx_{\perp}} = 2 \frac{\alpha_s}{\pi} Q^2 T x_{\perp} \left\{ \frac{T}{T'(1-T)y_1} [\rho(T', x_2^+, x_3^-) + \rho(T', x_2^-, x_3^+)] + \frac{1}{(1-T)y_2} \rho(x_1^+, x_2^-, T) \right\}, \quad (19)$$

where the function $\rho(T', x_2^{\pm}, x_3^{\pm})$ contributes to the summary distribution for the value

$$\begin{aligned}
T_0 \leq T \leq T_K, & \quad x_1^{(4)} \leq x_1 \leq x_1^{(1)}, \\
T_K \leq T \leq T_C, & \quad x_1^{(4)} \leq x_1 \leq x_1^{(3)}, \\
T_C \leq T \leq T_A, & \quad 0 \leq x_1 \leq x_1^{(3)},
\end{aligned} \tag{20}$$

while $\rho(T, x_2^+, x_3^-)$ and $\rho(x_1^+, x_2^-, T)$ contribute to the summary distribution for the values (16) and (12), respectively.

In Fig.3 dependence of the differential cross section (19) on the transverse momentum at some values of η is presented for the considered case of $T = 0.8$. The form of curves implies, that taking the mass of quarks into account noticeably changes the picture. Apart from the considerable expansion of the variation ranges of x_1 at $\eta \neq 0$ as compared with the massless case and the shift of these ranges towards small values of x_1 , it is remarkable that there appear structures in the curves.

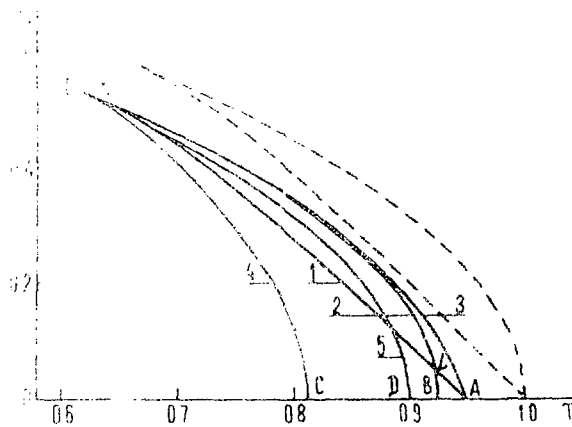
At $\eta = 0.1$ in the range $0.124 \approx x_1^{(4)} \leq x_1 \leq x_1^{(1)} \approx 0.275$, as it is seen in Fig.2, the summary distribution is due to events from the regions II and III only. Beginning from $x_1 \approx 0.275$ events in the region I become possible which results in a sharp increase of the cross section (almost an order of magnitude). Structure at $x_1 = x_1^{(3)} \approx 0.316$ has a kinematic nature and is due to the fact that at drawing nearer to the upper boundary of the region III ($x_1 \rightarrow x_1^{(5)}$) in the denominator of the expression (19) $y_2 \rightarrow 0$ (integrable square root singularity, connected with the phase volume in the region III). Beginning from this value the summary distribution is due to the regions I and II and beginning from $x_1 = x_1^{(2)} \approx 0.342$ - the region I only. At the boundary of the region I ($x_1 \rightarrow x_1^{(3)}$), there is again the square root singularity connected with the phase volume ($y_1 \rightarrow 0$) which leads to unlimited increase of the cross section.

At $\eta = 0.2$, in contrast to the case with $\eta = 0.1$, there are no events in the region III , therefore the corresponding structure ($y_2 \rightarrow 0$) does not appear. At $\eta = 0$, as it has already been mentioned, the variation range of x_1 is the same for all the regions and besides, $y_1 = y_2$, i.e. there is only one square root singularity at the common boundary of the regions. This is the reason why the distribution curve is continuous in this case.

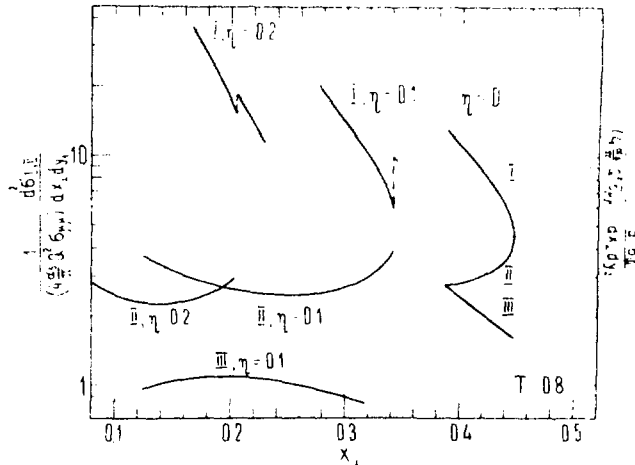
As the masses of heavy quarks are noticeably different, the corresponding values of η at a given energy of reaction, being in a square-law dependence with them, will be quite different too. Taking into account, that at a given T the region of the admissible values of x_1 significantly depends on η , one might suppose that the measuring of T and x_1 would allow to judge about the flavour of the quark or antiquark, responsible for the given event.

The results obtained in this paper can be used in the corresponding Monte-Carlo calculations with the use of various models for fragmentation process of quarks and gluons into hadrons.

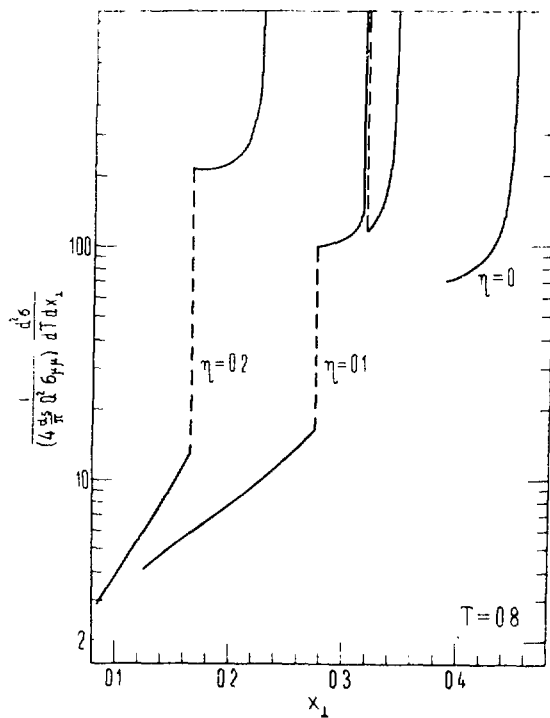
The author thanks S.G. Matinyan for discussion.



1. The phase space of the considered process in variables (T, α_1) at $\eta = 0.1$. The dashed line indicates the phase space at $\eta = 0$, which is the same for all three regions I - III.



2. The dependence of the cross section $d^2\sigma/d\alpha_1 dy$, normalized to the value $4 \frac{\alpha_s}{\pi} Q^2 \sigma_{\mu\mu}$, on the transverse momentum in three different regions I-III in case of $\Gamma = 0.8$, at some values of the mass parameter η .



3. The dependence of the cross section $d^2\sigma/dTdx_1$ of the considered process on the transverse momentum at the same parameters as in Fig.2.

REFERENCES

1. Farhi E. Quantum Chromodynamics Test for Jets. - Phys.Rev. Lett., 1977, vol. 39, p. 1587.
2. De Rujula A., Ellis J., Floratos E.G., Gaillard M.K. QCD Predictions for Hadronic Final States in e^+e^- Annihilation. - Nucl.Phys., 1978, vol. B138, p. 387.
3. Hoyer P., Osland P., Sander H.G. et al. Quantum Chromodynamics and Jets in e^+e^- . - Nucl.Phys., 1979, vol. B161, p. 349.
4. Shakhnazaryan Yu.G. Transverse Momentum Distribution of the Three-Jet Event Cross Section in e^+e^- Annihilation. - Preprint EPI - 728(43) - 84, Yerevan, 1984.
5. Ioffe B.L. Associated Production of Gluonic Jets and Heavy Mesons in e^+e^- Annihilation. - Phys.Lett., 1978, vol. 78B, p. 277.
6. Granberg G., Ng Y.T., Tye S.-H.H. Angular Distributions of Heavy-Quark Jets in e^+e^- Annihilation. - Phys.Rev., 1980, vol. D21, p. 62.
7. Kramer G., Schierholz G., Willrodt J. Cross Sections and Angular Distributions of Three-Jet Final States in e^+e^- Annihilation for Heavy Quarks. - DESY preprint 79/69, 1979.
8. Шахназарян Ю.Г. Распределение по T трехструйных событий в e^+e^- -аннигиляции для тяжелых кварков.-ЯФ,1982, т.35, с.438.

The manuscript was received 22 January 1986

Ю.Г.ШАХНАЗАРЯН

РАСПРЕДЕЛЕНИЕ ПО ПОПЕРЕЧНОМУ ИМПУЛЬСУ СЕЧЕНИЯ ПРОЦЕССА $e^+e^- \rightarrow$
 $\rightarrow q\bar{q}g$ ДЛЯ ТЯЖЕЛЫХ КВАРКОВ

(на английском языке, перевод Г.А.Папяна)

Редактор Л.П.Мукаян

Технический редактор А.С.Абрамян

Подписано в печать 21/IV-86г. ВФ-06576 Формат 60x84/16
Офсетная печать. Уч.изд.л.0,8 Тираж 299 экз.Ц.10 к.
Зак.тип.№ 252 Индекс 3624

Отпечатано в Ереванском физическом институте
Ереван 36, Маркаряна 2

индекс 3624



ЕРЕВАНСКИЙ ФИЗИЧЕСКИЙ ИНСТИТУТ